

Dynamic Negative Bias Temperature Instability and Comprehensive Modeling in PMOS Body-Tied FinFETs

Hyunjin Lee, Choong-Ho Lee*, Donggun Park* and Yang-Kyu Choi

Dept. of EECS, Korea Advanced Institute of Science and Technology, Daejeon 305-701, Korea

*Device Research Team, Semiconductor R&D Division, Samsung Electronics Co., Kyunggi-Do 449-711, Korea

Email: jinlee@eeinfo.kaist.ac.kr, Phone: +82-42-869-5477, Fax: +82-0505-869-3477

Abstract

This paper presents a novel approach to estimate the rising and falling behavior of N^{th} -order on-state current by dynamic negative bias temperature instability (DNBTI). For the first time, a modified DNBTI model in PMOS body-tied FinFETs was proposed and compared with experimental data. The approach can provide a quick estimation of periodic DNBTI behavior by stress and recovery. The DNBTI behaviors dependent upon stress bias, fin width, body temperature, and substrate bias were analyzed. The proposed model closely matched with the measured static-lifetime.

Introduction

Multi-gate FinFET structures have strengths of high robustness on short-channel effects and superior scalability using conventional processes [1,2]. However, due to the scalability, NBTI starts to limit the device reliability of digital and analog circuits [3,4]. Previous studies indicate the improvement on NBT-stress with a wide fin width (W_{Fin}) in the SOI as well as in the body-tied FinFETs because of the hole concentration reduction at the Si-SiO₂ interface [5,6]. Recently, recovery of the NBTI has become a concern for the AC-lifetime prediction [7,8].

Experiments

Detailed fabrication processes of body-tied FinFETs have already been reported [2]. For the dynamic BT-stress, negative biases ($V_G=V_{\text{TO}}-V_{\text{Stress}}$) for stress-states and positive biases ($V_G=V_{\text{TO}}+V_{\text{Stress}}$) for recovery-states were applied to the gate of body-tied FinFETs for 100 sec. Additionally, the source, drain and substrate were grounded with various Temp: 50°C, 80°C, 125°C, and 150°C. A V_{sub} of -0.2 V was applied to ensure the virtual-floating body effects, even in the body-tied FinFETs, which can mimic SOI FinFETs [4]. To investigate the fin width dependence of DNBTI behaviors, W_{Fin} of 30 nm, 50 nm, and 100 nm were used with a gate length of 100 nm and a gate oxide thickness of 1.7 nm. The DNBTI monitoring scheme was reported in ref. [5].

Results and Discussions

The on-current (I_{ON}) degradation and enhancement of the PMOS body-tied FinFETs are shown in Fig. 1 with various DC stress biases (V_{Stress}). I_{ON} degradation represents an increment of N_{it} and N_{ot} by Si-H bond breaking; furthermore, its enhancement represents N_{ot} neutralization and N_{it} re-passivation. [7,9]. To achieve an analytical and comprehensive understanding of DNBTI with V_{Stress} , Temp, W_{Fin} , and floating body effects, a previous model [10] was revamped with fitting parameter, κ .

Fig. 2 shows I_{ON} variation on stress- and recovery-states. After the 1st stress, n was 0.25; n was then reduced to ± 0.05 after the 1st recovery and the 2nd stress. The coefficient $n=0.25$ comes from the diffusion mechanism, which is the same value of planar bulk-devices [10], and the reduction of n ($= 0.05$) comes from the lock-in mechanism [7]. Fig. 3 shows that the exponent, n , was independent from W_{Fin} (30nm~100nm), V_{Stress} (2.4 V~3.4 V), Temp (50°C, 125°C), and V_{sub} (0 V, -0.2 V). Fig. 4 and Fig. 5 show the Y_1 -intercept of the 1st stress using Eq. 2 and the I_{ON} degradation versus $-1/k_{\text{B}}T$ to extract E_a using Eq. 4. The coefficient m is affected by V_{sub} but not by W_{Fin} , when the E_a decreases with the increment of W_{Fin} and V_{sub} . Fig. 6 shows the exponents for the E_{ox} , such as m_1 ($V_{\text{sub}}=0$ V, FinFET); m_2 ($V_{\text{sub}}=-0.2$ V, FinFET); and m_3 (single-gate bulk-FET), and the activation energy of the body-tied FinFETs and the single-gate bulk-FETs, which correspond to an infinite fin width. m did not show W_{Fin} dependency, but they were dependent on V_{sub} . Comparing m_3 and $m_{1,2}$, an increase was seen as the number of gates increased, i.e., $m_{1,2} > m_3$ [10,11]. E_a was larger in

the single-gate bulk planar MOSFETs than in the body-tied FinFETs [8,10-13]. E_a decreased as the W_{Fin} decreased and a negative V_{sub} was applied. Table 1 summarizes the extracted coefficients, A , n , m , and E_a after the 1st stress. The virtual floating body formed by applying $V_{\text{sub}}=-0.2$ V resulted in the decrement of m and E_a . Decrement of E_a caused more degradation of the device performance. Fig. 7 shows the ΔI_{ON} at $V_{\text{sub}}=0$ V and -0.2V. The cross point of ΔI_{ON} between $A(E_{\text{ox}})^m$ and $\exp(-E_a/k_{\text{B}}T)$ represents that E_a is dominant at a low E_{ox} field and that m is dominant at a high E_{ox} field. The virtual floating device shows worse device performance in the low E_{ox} region, i.e., in the E_a dominant region. However, the virtual floating device shows better device performance in the high E_{ox} region, i.e., in the m dominant region. Since an actual operative region of the device is at a low E_{ox} , the NBTI is worse at a SOI than at a bulk substrate, which is consistent with a previous report [5].

Fig. 8 shows an estimation of the I_{ON} variation using the measured data under the DNBT-stress. Guidelines of $\Delta I_{\text{ON}}/I_{\text{ON},0}$ under the NBT-stress are increased according to t^n , the power time law. One guideline after the 1st stress was extracted from $t_{s,1}$ and $t_{s,2}$, and it was proportional to the exponent, $n=0.25$. Similarly, the other guideline was extracted from $t_{s,2}$ and $t_{s,3}$, and it was proportional to the exponent, $n=0.05$. At the N^{th} -order, $\Delta I_{\text{ON}}/I_{\text{ON},0}$ follows the guideline of the 2nd stress [14]. Periodic $\Delta I_{\text{ON}}/I_{\text{ON},0}$ behavior after the N^{th} -order stress and recovery is well matched with the proposed DNBTI modified model (Eq. 1) by using parameters in Table 1, the 1st stress measurement data, the 1st and the 2nd guidelines from the 1st and 2nd stress measurement data, and the fitting parameter, κ . The solid lines of Fig. 9(a)(b) represent the DNBTI profiles modeled using the proposed method. Even using the 1st and 2nd stress-state measurement data, the modeled N^{th} -order stress and recovery profiles are well matched with the measurement results. The stress bias effects show a different value of κ due to the different E_{ox} dominant region. Fig. 10 shows the static-lifetime predicted by the modified DNBTI model at $W_{\text{Fin}}=50$ nm & 100 nm and $V_{\text{sub}}=0$ V & -0.2 V with different V_{Stress} . The device static-lifetime is defined at 10% of the drain saturation current. The root-mean square error of measured lifetime (τ_{me}) and modeled lifetime (τ_{mo}) was approximately 16% (Eq. 5).

Conclusions

A modified DNBTI model and extraction method were developed to predict the N^{th} -order DNBTI profile with various V_{Stress} , Temp, W_{Fin} , and V_{sub} . The stress time exponent, n , was 0.25 at the 1st stress-state and was changed to ± 0.05 after the 1st recovery-state. A decrement of E_a with a narrower W_{Fin} represented the increment in N_{it} and device degradation. A virtual floating body indicated a decrement of the coefficients m and E_a . The modeled static-lifetime coincided well with the measured static-lifetime, showing a root-mean square error of 16%.

References

- [1] Y.-K. Choi et al., *IEDM*, p.421, 2001. [2] T. Park et al., *VLSI*, p.135, 2003. [3] V. Reddy et al., *IRPS*, p.248, 2002. [4] C. Schliinder et al., *IRPS*, p.5, 2003. [5] H. Lee et al., *EDL*, Vol.26, p.326, 2005. [6] H. Kufluoglu et al., *IEDM*, p.113, 2004. [7] S. Rangan et al., *IEDM*, p.341, 2003. [8] V. Huard et al., *IRPS*, p.40, 2004. [9] S. Tsujikawa et al., *VLSI*, p.139, 2003. [10] S. Ogawa et al., *Phys. Review B*, Vol.51, p.4218, 1995. [11] M. Houssa et al., *IEDM*, p.121, 2004. [12] G. Haller et al., *J. Appl. Phys.*, Vol.56, p.1844, 1984. [13] N. Kimizuka et al., *VLSI*, p.92, 2000. [14] Y. Mitani et al., *IEDM*, p.117, 2004.

$$\Delta I_{ON} = A \kappa t^n (E_{ox})^m \exp(-E_a/k_B T) \dots \text{Eq. 1}$$

$$\log(\Delta I_{ON}) = n \log(t) + Y_1 \dots \text{Eq. 2}$$

$$Y_1 = m \log(E_{ox}) + Y_2 \dots \text{Eq. 3}$$

$$\log(\Delta I_{ON}) = E_a(-1/k_B T) + Y_3 \dots \text{Eq. 4}$$

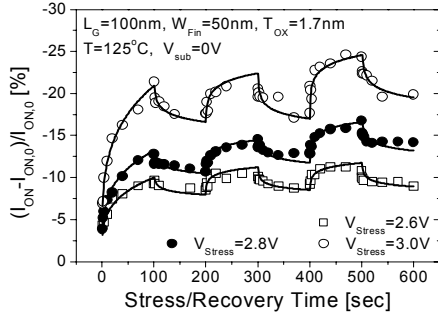


Fig. 1. I_{ON} degradation and enhancement versus stress/recovery time for different dynamic NBT-stress and PBT-stress biases.

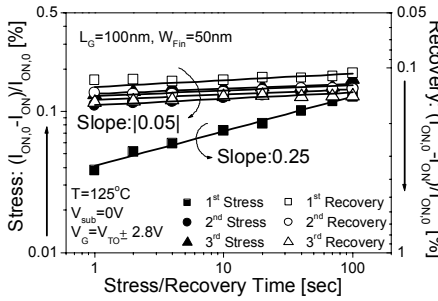


Fig. 2. I_{ON} degradation and enhancement with a number of stress- and recovery-states. After the 1st stress, n is fixed to 0.25 and reduced to ± 0.05 after the 1st recovery and the 2nd stress.

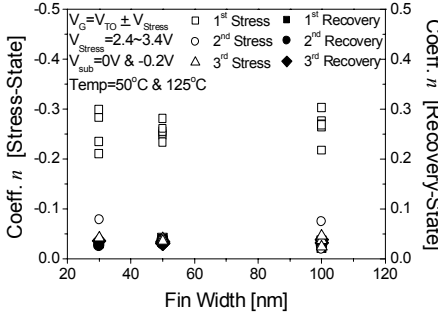


Fig. 3. The coefficient n vs. W_{Fin} with various stress and recovery states. The 1st stress n is fixed to the range of 0.2~0.3, and the n of the other states are fixed to the range of |0~0.1|.

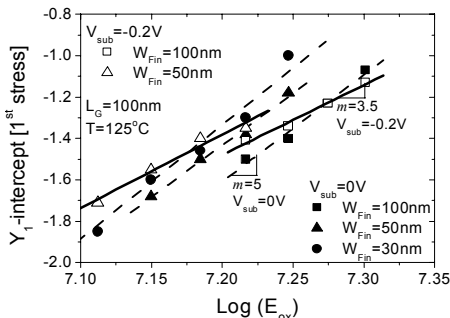


Fig. 4. Y_1 -intercept of the 1st stress from Eq. 3 versus E_{ox} with various W_{Fin} and V_{sub} . The coefficient m shows no W_{Fin} dependency, but does show V_{sub} dependency.

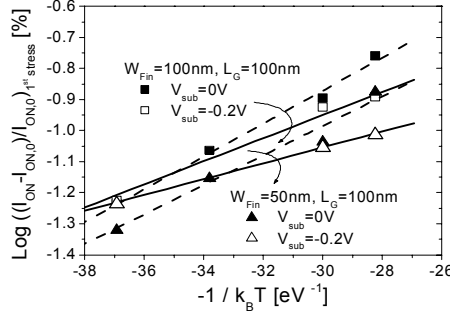


Fig. 5. I_{ON} degradation versus $-1/k_B T$ to find the coefficient E_a , the activation energy. E_a decreases with the increment of fin width and as the substrate bias is applied.

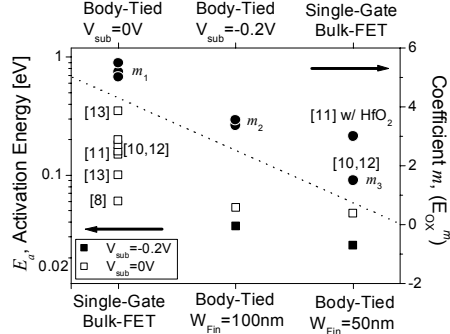


Fig. 6. Right and top axis shows m for a single-gate and body-tied FinFETs ($V_{sub}=0$ V and -0.2 V). Left and bottom axis shows E_a of the body-tied FinFETs with a W_{Fin} of 50 nm and 100 nm, and a single-gate bulk-FET (infinite W_{Fin}).

W_{Fin}	V_{sub}	A	n	m	E_a
100nm	0V	2×10^{-37}	0.25 ± 0.05	5	0.053eV
	-0.2V	1×10^{-26}	0.25 ± 0.05	3.5	0.037eV
50nm	0V	2×10^{-37}	0.25 ± 0.05	5	0.048eV
	-0.2V	1×10^{-26}	0.25 ± 0.05	3.5	0.025eV
Bulk FET	-	-	0.25	1.5	0.06eV~0.35eV

Table 1. Extracted coefficients A , n , m , and E_a after the 1st stress with $W_{Fin}=50$ nm, 100 nm and $V_{sub}=0$ V, -0.2 V. E_a shows W_{Fin} dependency, and A , m , and E_a show V_{sub} dependence.

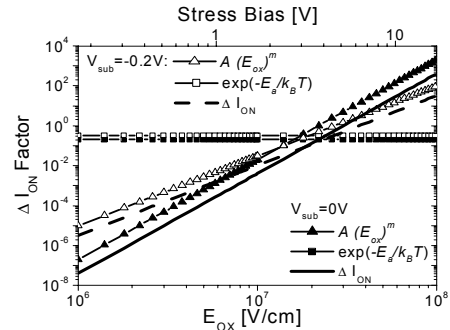


Fig. 7. I_{ON} factors versus E_{ox} for different substrate biases. The E_{ox} dependency of the floating body effect is the correlated results of the factor $A(E_{ox})^m$ and $\exp(-E_a/k_B T)$. The NBTI of the SOI FinFETs was worse than that of the body-tied FinFETs in the low E_{ox} region [5].

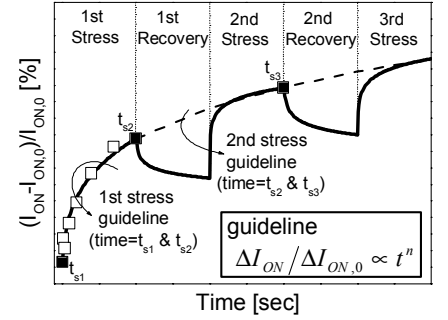


Fig. 8. Periodic $\Delta I_{ON}/I_{ON,0}$ under DNBT-stress. The 1st stress guideline increased according to t^n with $n=0.25$, and changed to $n=0.05$ after the 2nd stress.

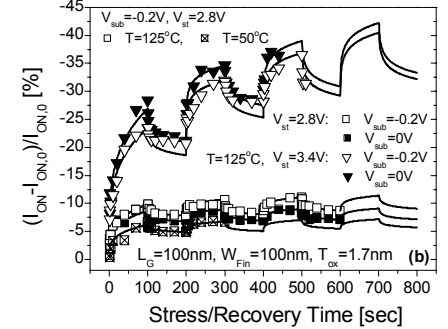
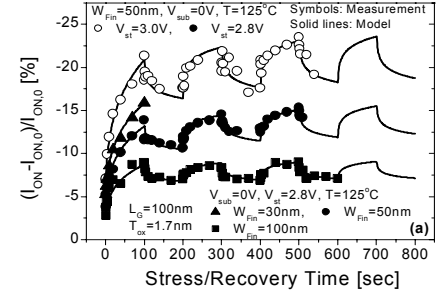


Fig. 9. $I_{ON}/I_{ON,0}$ of DNBTI versus stress/recovery time with various (a) V_{Stress} , W_{Fin} , (b) Temperature and V_{sub} . Solid lines represent the DNBTI profiles modeled using the proposed method.

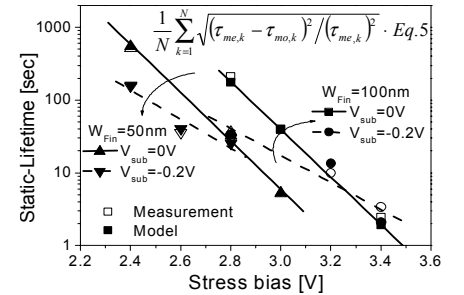


Fig. 10. Measured and modeled static-lifetime at $W_{Fin}=50$ nm, 100 nm and $V_{sub}=0$ V, -0.2 V versus V_{Stress} according to Eq. 1 and the parameters in Table 1. The root-mean square error is 16%.

Acknowledgment

This work was supported in part by Samsung Electronics Co., Ltd., and in part by the National Research Program for the 0.1-Terabit Nonvolatile Memory Development, sponsored by the Korea Ministry of Science and Technology.